Received: 4 April 2020 | Revised: 23 September 2020 | Accepted: 28 September 2020

DOI: 10.1096/fj.202000761RR

RESEARCH ARTICLE

THE FASEB JOURNAL

Loss of ARNT in skeletal muscle limits muscle regeneration in aging

Yori Endo[1] | Kodi Baldino[1] | Bin Li[1,2] | Yuteng Zhang[1,2] | Dharaniya Sakthivel[3] | Michael MacArthur[4,5] | Adriana C. Panayi[1] | Peter Kip[5] | Daniel J. Spencer[6] | Ravi Jasuja[6] | Debalina Bagchi[7] | Shalender Bhasin[6] | Kristo Nuutila[1] | Ronald L. Neppl[7] | Amy J. Wagers[8,9,10] | Indranil Sinha[1,9]

[1]Division of Plastic Surgery, Brigham and Women's Hospital, Harvard Medical School, Boston, MA, USA

[2]Department of Plastic and Aesthetic Surgery, Nanfang Hospital, Southern Medical University, Guangzhou, China

[3]Division of Human Genetics, Baylor College of Medicine, Houston, TX, USA

[4]Department of Genetics and Complex Diseases, Harvard School of Public Health, Boston, MA, USA

[5]Division of Vascular and Endovascular Surgery, Brigham and Women's Hospital, Boston, MA, USA

[6]Division of Endocrinology, Brigham and Women's Hospital, Boston, MA, USA

[7]Department of Orthopedic Surgery, Brigham and Women's Hospital, Harvard Medical School, Boston, MA, USA

[8]Joslin Diabetes Center, Boston, MA, USA

[9]Harvard Department of Stem Cell and Regenerative Biology, Harvard Stem Cell Institute, Cambridge, MA, USA

[10]Paul F. Glenn Center for the Biology of Aging, Harvard Medical School, Boston, MA, USA

Correspondence
Indranil Sinha, Division of Plastic Surgery, Brigham and Women's Hospital, 45 Francis Street, Boston, MA 02115, USA.
Email: isinha@bwh.harvard.edu

Funding information
HHS | NIH | National Institute on Aging (NIA), Grant/Award Number: K76AG059996 and P30AG031679; National Institute of Diabetes and Digestive and Kidney Diseases, Grant/Award Number: P30 DK036836; Glenn Foundation for Medical Research

Abstract

The ability of skeletal muscle to regenerate declines significantly with aging. The expression of aryl hydrocarbon receptor nuclear translocator (ARNT), a critical component of the hypoxia signaling pathway, was less abundant in skeletal muscle of old (23-25 months old) mice. This loss of ARNT was associated with decreased levels of Notch1 intracellular domain (N1ICD) and impaired regenerative response to injury in comparison to young (2-3 months old) mice. Knockdown of ARNT in a primary muscle cell line impaired differentiation in vitro. Skeletal muscle-specific ARNT deletion in young mice resulted in decreased levels of whole muscle N1ICD and limited muscle regeneration. Administration of a systemic hypoxia pathway activator (ML228), which simulates the actions of ARNT, rescued skeletal muscle regeneration in both old and ARNT-deleted mice. These results suggest that the loss of ARNT in skeletal muscle is partially responsible for diminished myogenic potential in aging and activation of hypoxia signaling holds promise for rescuing regenerative activity in old muscle.

Abbreviations: ARNT, aryl hydrocarbon receptor nuclear translocator; CSA, cross-sectional area; DAPT, N-[N-(3,5-difluorophenacetyl)-l -alanyl]-S-phenylglycinenonbreakingspacet-butyl ester; DPI, days postinjury; FGF, fibroblast growth factor; HIF, hypoxia inducible factor; HSA, human α-skeletal actin; N1ICD, notch1 intracellular domain; SMP, skeletal muscle precursors; TA, tibialis anterior.

[Correction added on September 16, 2020, after first Onlinepublication: Ronald Neppl and Debalina Bagchi affiliation 7 has been updated and Fig 9B missing p-value has been updated].

KEYWORDS

aging, hypoxia signaling, muscle regeneration

1 | INTRODUCTION

Skeletal muscle precursors (SMPs), a subpopulation of muscle satellite cells, are stem cells which are responsible for muscle regeneration following injury.[1] Although skeletal muscle is one of the few tissues that maintain a lifelong capacity to regenerate, its myogenic potential and regenerative response following injury dramatically decline with aging.[2] Hypoxia inducible factor (HIF)-1α is a master transcriptional regulator of the hypoxia signaling pathway and is known to promote satellite cell self-renewal,[3] particularly in aging.[4] Separately, previous studies have shown that HIF-1α promotes Notch activity,[5] which is required for robust muscle regeneration and diminishes with aging.[6] Furthermore, deletion of Notch ligands in the skeletal muscle stem cell niche results in decreased number of stem cells and impaired myogenesis.[7,8] Indeed, combined loss of HIF-1α and HIF-2α within muscle stem cells limits the skeletal muscle Notch signaling and myogenic potential.[9] However, the regulation of the hypoxia pathway itself in response to injury and during the regenerative period has not been previously examined.

To evaluate the complex role of hypoxia signaling in myogenesis, particularly with regards to its age-related impairment, we assessed the regulation of HIFs within young and old skeletal muscle in mice. We discovered an aging-associated loss of skeletal muscle aryl hydrocarbon receptor nuclear translocator (ARNT, also known as HIF-1β). ARNT is a central factor in hypoxia signaling and its binding to both HIF-1α and HIF-2α in the cytoplasm is required for the nuclear translocation of these proteins. Within the nucleus, the heterodimer of ARNT and HIF-1α, or ARNT and HIF-2α, binds to the hypoxia response element and induces transcriptional activity.[10,11] Initially, ARNT was thought to be constitutively expressed,[12] but more recent studies have shown in multiple tissue types that ARNT is dynamically regulated and responds to stimuli.[13] Despite its critical role in hypoxia signaling, ARNT regulation during aging or muscle regeneration has not been previously characterized.

We found that skeletal muscle's regenerative response to injury was significantly impaired in old mice, with much lower levels of ARNT and nuclear HIF-1α following injury, in the context of similar HIF-1α cytosolic levels within the whole muscle. In addition, substantially less Notch1 intracellular domain (N1ICD) was found in old muscle, consistent with what others have previously shown.[14] siRNA knockdown of ARNT limited hypertrophy in a primary muscle cell line. Similarly, skeletal muscle-specific knockout of ARNT in young, adult mice resulted in diminished muscle regeneration with a corollary decrease in N1ICD levels. Importantly, SMPs harvested from these mice demonstrated normal rates of differentiation and frequency. Restoration of HIF-1α nuclear translocation by a pharmacological activator of hypoxia signaling, ML228, enhanced N1ICD levels in the whole muscle and accelerated muscle regeneration following injury in old mice. This study revealed a dynamic role of ARNT in regulating the hypoxia signaling pathway during muscle regeneration, highlighting its critical role in myogenesis. Supplementation of ARNT activity may, therefore, restore the capacity of resident muscle stem cells, enhancing muscle repair in aged muscle.

2 | MATERIALS AND METHODS

2.1 | Animals

All animal procedures were approved by the Institutional Animal Care and Use Committee of Brigham and Women's Hospital, and were conducted within the guidelines of the US National Institutes of Health. Young C57BL/6 mice (10-12 weeks of age) were obtained from Jackson Laboratories. Old C57BL/6 mice were obtained from the National Institute of Aging. $ARNT^{fl/fl}$ mice (a kind gift from F. Gonzalez) and human α-skeletal actin (HSA)-Cre ER mice (a kind gift from W. Kaelin) were bred in house. To investigate the role of ARNT in muscle regeneration, we utilized an inducible Cre-lox murine model. We generated a genetically modified mouse line by crossing $ARNT^{fl/fl}$ mice with the temporally regulatable, skeletal muscle-expressed human skeletal actin (HSA)-Cre ER transgene. We generated (a) $ARNT^{fl/fl}$ mice without the Cre ER recombinase, which were utilized as a control, and (b) experimental HSA-Cre ER $ARNT^{fl/fl}$ mice. For the activation of these mice, Tamoxifen (0.1 mg/g body weight, Sigma Aldrich, St. Louis, MO, USA) or corn oil vehicle (10 uL/g body weight) was injected for five consecutive days. Experimentation began 7 days following the last injection. For ML228 treatment, ML228 (TOCRIS #1357171-62-0, Cayman Chemical, Ann Arbor, MI, USA) was dissolved in DMSO (0.03 mg ML228 in 1 mL DMSO) and was injected intraperitoneally (0.1 mL) once daily for a total of 5 days. For *N*-[*N*-(3,5-difluorophenacetyl)-L-alanyl]-*S*-phenylglycine *t*-butyl ester (DAPT) treatment, DAPT (#26-345-0, Fisher Scientific, Waltham, MA) was dissolved in DMSO and was injected at a dose of 125 mg/kg body weight once daily,[15] for a total of 5 days, similar to ML228. DMSO (vehicle only) was used as a negative control. Cryoinjury was induced on

the left legs of the animals immediately following the second injection of DMSO, ML228, DAPT, or DAPT and ML228 approximately 24 hours following the first injection. The animals were housed at the Brigham and Women's Hospital Animal Care Facility and were given ad libitum access to food and water.

2.2 | Muscle cryoinjury and quantification of regenerating myofibers

All mice were anesthetized using isoflurane and the skin anterior to the tibialis anterior (TA) muscle was prepped with sterile alcohol. A skin incision was made and the TA was exposed. A metal probe cooled in dry ice was placed on the skin for 10 seconds, creating a cryoinjury. The skin incision was closed immediately after injury. This procedure generates a reproducible injury in the muscle with a discrete border between uninjured and injured muscle. Injured muscles were allowed to recover for 5 or 10 days before harvest. To quantify the area of regeneration, 10 photos per sample were taken spanning the entire regenerating area in cross section, and the area of 12 to 15 regenerating myofibers (identified by their centrally located nuclei) were measured in each image using ImageJ. This collectively resulted in a total of approximately 150 myofiber areas for each sample.

2.3 | Histology and immunostaining

Muscles were fixed in 4% of paraformaldehyde, washed in PBS and stored in 70% of ethanol for paraffin embedding. Hematoxylin and eosin (H&E) staining was used to visualize regenerating myofibers. Newly formed myofibers were identified by their centrally located nuclei. For immunostaining, skeletal muscle sections were blocked with Blocker BSA (#37520, ThermoFisher, Waltham, MA, USA), and stained with antibodies against CD31 (1:100, #ab7388, Abcam) and Laminin (1:100, #ab11571, Abcam, Cambridge, UK). Separately, C2C12 cells and satellite cells were stained with antibodies against myosin heavy chain 4 (MF20) (1:100, #14-6503-82, ThermoFisher). Secondary antibodies used were (1:400, #A21470, ThermoFisher) and (1:400, #A11037, ThermoFisher), respectively. Bright field and fluorescent images were acquired using an Olympus BX53 microscope.

2.4 | Satellite cell isolation

Myofiber-associated cells were prepared from two-step collagenase/dispase digestion of intact limb muscles (Abdominals, extensor digitorum longus, gastrocnemius, quadriceps, soleus, TA, and triceps brachii), as previously described.[15] All cells were incubated in Hank's Buffered Salt Solution (Gibco) containing 2% of Fetal bovine calf serum on ice for 20 minutes using the following antibodies: anti-mouse CD45 (1:200, clone 30-F11, BioLegend, San Diego, CA, USA, #103106 for PE conjugate); anti-mouse/human CD11b (1:200, clone M1/70, BioLegend #101208 for PE conjugate); anti-mouse Ter119 (1:200, BioLegend Cat#116208 for PE conjugate); APC conjugate anti-Ly-6A/E (Sca-1) (1:200, clone D7, BioLegend #108112); anti-mouse Integrin alpha 7 Antibody, Novus Biologicals #3C12); biotinylated anti-mouse CD184 (CXCR4) (1:100, BD Pharmingen #551968); and PE/Cy7 conjugate anti-streptavidin (1:100, eBioscience, San Diego, CA, USA, #25431782). Muscle satellite cells were identified as the CD45-Sca-1- CD11b- Ter119- CXCR4+ β1-Integrin+ cell population. Cells were sorted by Fluorescence-Activated Cell Sorting (FACS) using Aria II (BD Biosciences, Woburn, MA, USA), and live cells were identified as calcein blue-positive (1:1000, Invitrogen) and propidium iodide-negative (PI, 1 mg/mL, eBioscience).

2.5 | Myogenic differentiation assays

Sorted cells were plated at 1×10^4 cells/well in 96 well plates, which were pre-coated with 1 μg/mL rat-tail collagen (Sigma) and 10 μg/mL natural mouse laminin (Invitrogen). Cells were expanded for 5 days in growth medium (GM) composed of Ham's F10 (Invitrogen)+20% horse serum (Atlanta Biologicals, Flowery Branch, GA, USA) with 1% penicillin/streptomycin. A 5 ng/ml basic fibroblast growth factor (FGF) (Sigma Aldrich) was replaced daily. After 5 days, cells were re-plated onto chamber slides coated with collagen (Sigma) and laminin (Gibco) for 2 days in growth media. Medium was then switched to differentiation medium (DM) consisting of Ham's F10 + 2% horse serum + 1% penicillin/streptomycin. Cells were kept in DM for 6 days, then, medium was aspirated and cells were fixed with 4% of paraformaldehyde and processed for immunofluorescence. Nuclei per field counts were performed by counting DAPI stained nuclei in five distinct 10X fields. Fusion index was calculated as the ratio of the number of nuclei inside myotubes expressing myosin heavy chain to the total number of nuclei in a given field.

2.6 | Quantitative RT-PCR

To isolate whole muscle mRNA, muscle was homogenized using a Gentle MACS Dissociator (Miltenyi Biotech, Bergisch Gladbach, Germany) and RNeasy kit (Qiagen, Hilden, Germany), following the manufacturer's instructions. cDNA was prepared from mRNA using Superscript III Reverse Transcriptase Supermix Kit (Invitrogen, Carlsbad, CA). Real-time quantitative PCR reactions were carried out

in an ABI StepOnePlus machine, using SYBR Green PCR mix (Applied Biosystems, Foster City, CA). β-actin was used as a housekeeping gene, and gene expression levels were normalized to β-actin expression.

Total RNA from TA muscle and C2C12 cells was extracted using RNeasy Mini Kit (Qiagen) according to the manufacturer's instructions. cDNA was prepared from mRNA using SuperScript III First-Strand kit (Invitrogen). Real-time quantitative PCR reactions were carried out in ABI StepOnePlus machine, using SYBR Green PCR mix (ThermoFisher). The temperature profile used was 95 degrees for 0 minutes, then, 40 cycles of 95 degrees C, 60 degrees C, 72 degrees C each for 30 seconds. All the gene expression levels were normalized to β-actin. Primers sequences are provided below. Primers used are: ARNT: F: (5′ CGAGAATGGCTGTGGATGAG 3′) and R: (5′ GGATGGTGTTGGACAGTGTAG 3′), HIF-1α: F: (5′ AGCCCTAGATGGCTTTGTGA 3′) and R: (5′ TATCG AGGCTGTGTCGACTG 3′), HIF-2α: F: (5′ AATGACAGCT GACAAGGAGAAAAA 3′) and R: (5′ GAGTGAGTCAAAG ATGCTGTGTC 3′), mMyf5: F: (5′ TGAGGGAACAGGTG GAGAAC 3′) and R: (5′ AGCTGGACACGGAGCTTTTA 3′), MyoD: F: (5′ ACTTTCTGGAGCCCTCCTGGCA 3′) and R: (5′ TTTGTTGCACTACACAGCATG 3′), Myogenin: F: (5′ CTAAAGTGGAGATCCTGCGCAGC 3′) and R: (5′ GCA ACAGACATATCCTCCACCGTG 3′), and β-actin: F: (5′ CCTAAGGCCAACCGTGAAAA 3′) and R: (5′ AGCCATA CAGGGACAGCACA 3′).

2.7 | Protein quantification with immunoblotting and ELISA

Whole muscle lysates were isolated from TA muscles and subjected to subcellular fractionation (NE-PER Nuclear and Cytoplasmic Extraction Reagent Kit, Pierce, Franklin, MA, USA). Overall protein levels were quantified utilizing a BCA Protein Assay Kit (Pierce). Following subcellular fractionation, HIF-1α and ARNT were assessed in cytoplasmic and nuclear fractions through the use of ELISA (LS F4226 and LS-F10885).

For immunoblotting, proteins were separated on a 4%-12% of SDS-polyacrylamide gel with MOPS SDS Running Buffer (ThermoFisher) at 150 V. The gel was transferred onto an Immuno-Blot PVDF Membrane using the iBlot2 Dry Blotting System (ThermoFisher) for 7 minutes. The membranes were then blocked in blocking solution (Life Technologies, Carlsbad, CA) for 1 hour at room temperature then incubated with an antibody overnight at 4°C with constant shaking. The antibodies utilized were anti-cleaved Notch (Cell Signaling, Danvers, MA, USA, #4147) and anti-GAPHD (Cell Signaling #2118). To determine quality of fractionation, nuclear and cytoplasmic samples were additionally assessed for α-tubulin (Cell Signaling #2144) and histone H3 (Cell Signaling #4499). Following three 5-minutes washes in TBS-T buffer, the membranes were incubated with anti-rabbit IgG HRP-linked (Cell Signaling) secondary antibody. All the antibodies were diluted in blocking buffer. For immunodetection, the membranes were washed three times with TBS-T buffer, incubated with ECL solutions per manufacturer's specifications (Amersham Biosciences, Little Chalfont, UK) and exposed to Hyperfilm ECL. The membranes were stripped and re-probed with an antibody recognizing GAPDH for normalization. Band intensities were determined using ImageJ software.

2.8 | C2C12 culture

C2C12 cells were grown in Dulbecco's modified Eagle's medium (DMEM) supplemented with 10% heat-inactivated fetal bovine serum (FBS) and maintained at 37°C with 5% CO2 supply in a humidified incubator. At 75% confluency, cells were differentiated by adding DMEM supplemented with 2% horse serum for 5 days. Media was replaced every 24 hours during differentiation.

2.9 | siRNA transfection

For siRNA transfections, C2C12 cells were seeded in 6-well plates with or without coverslips and differentiated when 75% confluent. Cells were transfected every 24 hours from the day of adding the differentiation media referred to as Day 0 till Day 4 of differentiation. For each well, 150 uL of OPTI-MEM media (Life Technologies) was mixed with 3 μL of 10 uM siRNA (siControl or siArnt from Santa Cruz Biotechnology, Dallas, TX, ISA) and 9 μL of transfection reagent Lipofectamine RNAiMAX (Life Technologies) in separate tubes and incubated for 5 minutes. After 5 minutes, 150 μL of the constituent solutions from each tube were combined and incubated for another 30 minutes at room temperature to generate 300 μL of transfection mix. A 250 μL of the transfection mix were added per well to have a final siRNA concentration of 11 nM per well. Cells were collected from Day 0 (undifferentiated and nontransfected control) to Day 5. Cells were harvested every 24 hours after transfection in 1 mL TRIzol for RNA extraction or fixed on coverslips with 4% PFA for immunofluorescence staining.

2.10 | Laser Doppler

Laser Doppler perfusion imaging (LDPI) was performed using an LDPI analyzer (Moor Instruments, Devon, UK). Briefly, mice were kept under isoflurane anesthesia and mean LDPI flux intensity of the left hindlimb was measured at a rate of 4 ms/pixel. Data are presented as mean flux intensity across the hindlimb area.

2.11 | Statistical analysis

Data are presented as the mean and standard error. Statistical comparisons for normally distributed data were assessed for statistical significance using Student's *t*-test. Results comparing more than two groups were assessed by one-way ANOVA with Tukey's multiple comparison test (GraphPad Prism, GraphPad Software Inc, San Diego, CA, USA, RRID:

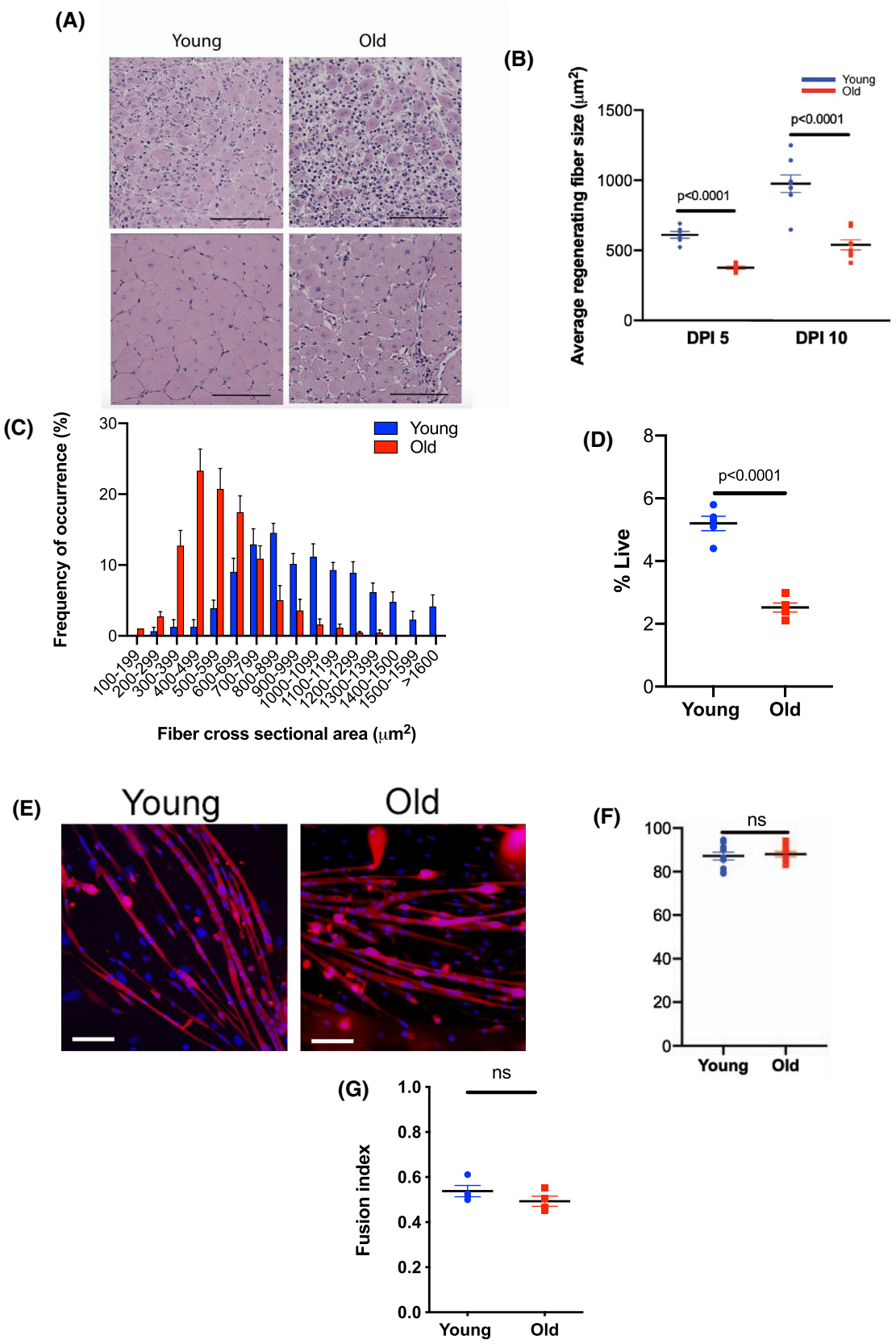

FIGURE 1 Regenerating muscle fiber size of old mice is smaller postinjury in association with a decline of ARNT levels. TA muscles of young (n = 5-8; 10-12 weeks old) and old (n = 5-8; 23-25 months old) mice were subjected to cryoinjury and the TA muscles were harvested for histological evaluation on DPI 5 and 10. (A) On average, young mice displayed larger regenerating fiber cross-sectional area compared to old mice on both DPI 5 and 10 (A,B). The distribution of regenerating muscle fiber size demonstrated a shift toward smaller cross-sectional areas in old mice, indicating a poorer regenerative response to injury on DPI 10 (n = 6 mice per group) (C). The frequency of SMPs, as a percentage of live cells with uninjured muscle, is less in old mice as compared to young mice (n = 6 per group) (D). Myosin heavy chain (MF20) expression was similar between the two groups following differentiation in a low-serum media for 5 days (E,F). Fusion index is similar between the two groups (G). Scale Bar: 200 μm

SCR_002798). The investigators were blinded to the experimental group assignments for outcome assessment. Statistical significance was accepted at $P < .05$.

3 | RESULTS

3.1 | Old mice display reduced skeletal muscle regeneration

Skeletal muscle regeneration in young (10-12 weeks) and old (23-25 months) mice was assessed by inducing cryoinjury in the tibialis anterior (TA) muscle, as previously described.[16] This injury modality causes necrosis and, subsequently, a localized regenerative response that can be reliably evaluated to assess and quantify new myofiber formation.[16,17] In young mice, cryoinjury induced an extensive regenerative response resulting in the formation of large, well-organized regenerating myofibers (Figure 1A-C). In contrast, the regenerative response in aged muscle was much less substantial, resulting in smaller and poorly organized regenerating myofibers (Figure 1A-C), with the average myofiber cross-sectional area (CSA) being 59% of that of young mice on day postinjury (DPI) 5 (618.0 ± 25.0 μm in young versus 366.0 ± 11.2 μm in old, $P < .001$) and 56% on DPI 10 (999.3 ± 58.5 μm in young versus 562.8 ± 33.1 μm in old, $P < .001$). In addition, the proportion of SMPs isolated by fluorescence-activated cell sorting within the pool of mononuclear cells was 60% lower in skeletal muscle harvested from old mice in comparison to young ($P < .001$), (Figure 1D). However, SMPs harvested from young mice and old mice both similarly underwent myogenic differentiation in culture, as evidenced by myosin heavy chain staining and fusion index (Figure 1E-G).

3.2 | ARNT levels are suppressed in old mice following injury

Recent studies have suggested that hypoxia signaling is required for the maintenance of SMPs' myogenic potential and thus muscle regeneration.[9] We therefore hypothesized that aging-associated dysregulation of hypoxia signaling might be one of the causes of limited skeletal muscle repair observed in aging. A focused hypoxia pathway PCR array demonstrated a global downregulation of hypoxia signaling factors and response genes in uninjured skeletal muscle of old mice compared to young (Supporting Figure S1). We next investigated whether HIFs, the transcriptional regulators of the hypoxia pathway, may be differentially regulated in aging to account for the observed decrease in the hypoxia response element gene expression. Skeletal muscle of old mice had significantly lower levels of cytoplasmic HIF-1α at baseline prior to injury (Figure 2A). Following injury, while cytoplasmic HIF-1α levels were similar in muscle of both young and old mice, lower levels of nuclear HIF-1α were found in muscle from old mice on DPI 5 compared to young (Figure 2A,B). These finding prompted us to investigate age-related changes in ARNT, as ARNT is necessary for the nuclear translocation of HIF-1α and HIF-2α.[10,11] We found that the ARNT levels in the cytoplasm were threefold lower in skeletal muscle of old mice in comparison to young mice at baseline ($P = .01$), as well as on DPI 5 ($P = .02$) and 10 ($P = .01$) (Figure 2C). No difference between young and old muscles was observed in the nuclear ARNT levels (Figure 2D). Nuclear and cytosolic fractionation was confirmed by immunoblotting for histone H3 and α-tubulin, respectively (Supporting Figure S1). Whole muscle ARNT gene expression was substantially decreased with aging (Figure 2E). Immunofluorescence demonstrated the presence of ARNT and HIF-1α within muscle fibers at baseline in old mice, which was a substantially less in comparison to young mice (Figure 2F).

HIF activity is thought to potentiate the Notch signaling pathway.[5] The activation of Notch1 results in the production of N1ICD, which translocates to the nucleus and regulates gene expression. Since ARNT is responsible for enabling the downstream signaling effects of both HIF-1α and HIF-2α, we hypothesized that ARNT regulates the skeletal muscle Notch activity. Indeed, N1ICD levels were found to be twofold lower in skeletal muscle from old mice in comparison to young in immunoblotting ($P = .001$) (Figure 2G,H).

The decrease in hypoxia signaling factors further prompted us to investigate if there were corollary changes in blood supply, which could account for the age-associated decline in skeletal muscle regeneration.[18] We measured capillary density in uninjured tibialis anterior muscle via

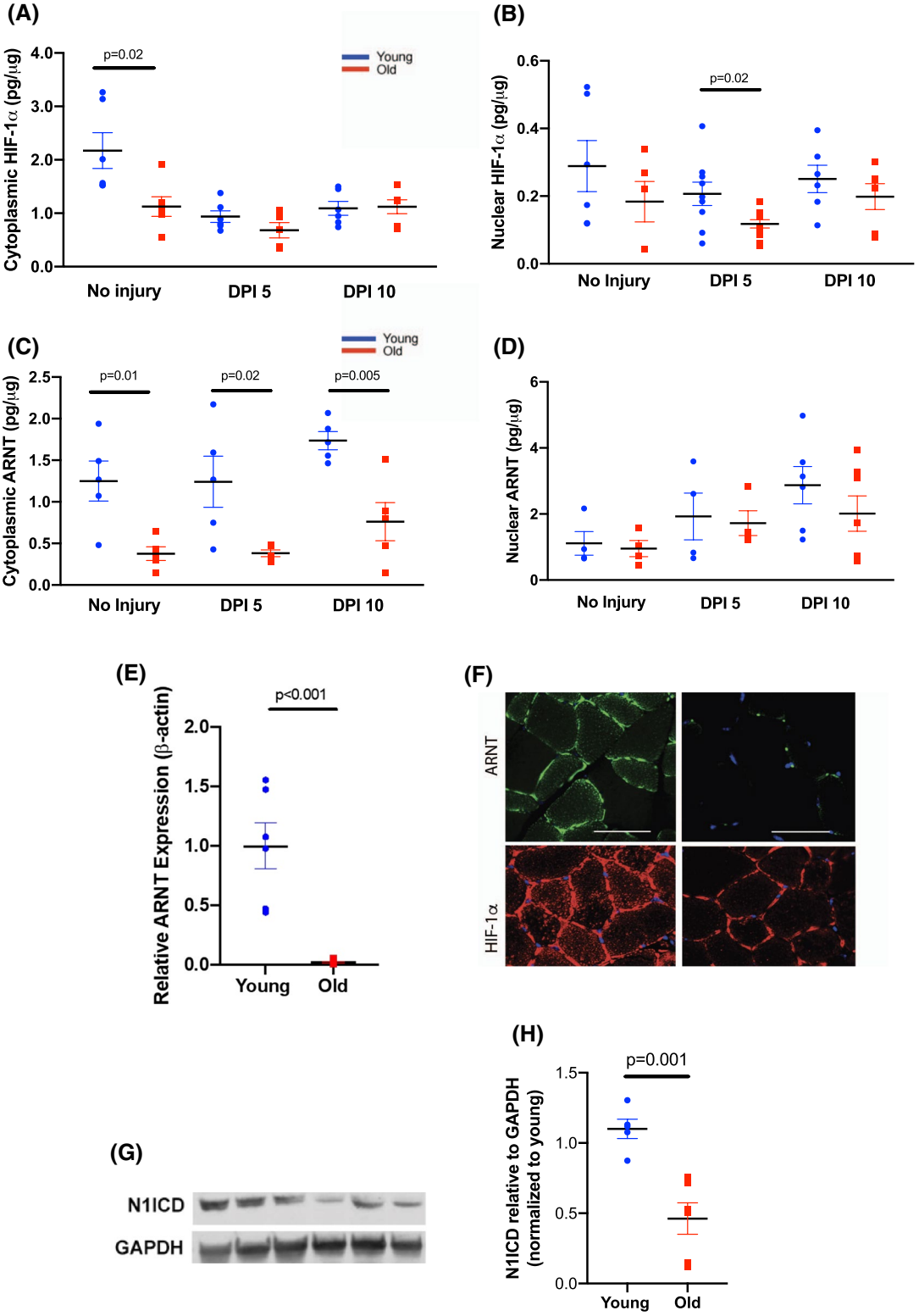

FIGURE 2 The hypoxia pathway is perturbed with aging. TA muscle of young (10-12 weeks old) and old (23-25 months old) mice underwent cryoinjury and were harvested on days 5 and 10 postinjury for histological analysis, enzyme-linked immunosorbent assay (ELISA), and PCR. Cytosolic HIF-1α levels were lower in old mice only prior to injury, whereas nuclear HIF-1α levels were found to be lower in old mice on DPI 5 (n = 6-9 per group, A,B). The levels of cytoplasmic ARNT protein were higher in young mice pre- and postinjury compared to old (C). Nuclear ARNT levels were similar in both groups (D) (n = 4-6 per group). ARNT gene expression was decreased in whole muscle with aging (n = 5 per group) (E). ARNT and HIF-1α immunofluorescence at baseline visualized a loss of ARNT and HIF-1α in old skeletal muscle, whereas the proteins were abundant in the muscle fibers of young muscle (F). Whole muscle N1ICD levels in skeletal muscle declined significantly with aging (G,H) (n = 4-6 per group). Scale Bar: 100 μm

CD31 immunofluorescence staining and observed no obvious differences between young and old mice (Figure 3A,B). However, blood flow rate at mid-thigh, measured by doppler ultrasound, was 30% lower in old mice as compared to young ($P = .04$) (Figure 3C,D). The baseline, uninjured skeletal muscle fiber CSA was similar between the two groups at the ages tested (Figure 3E,F). Given these data, we next sought to clarify how loss of ARNT in skeletal muscle

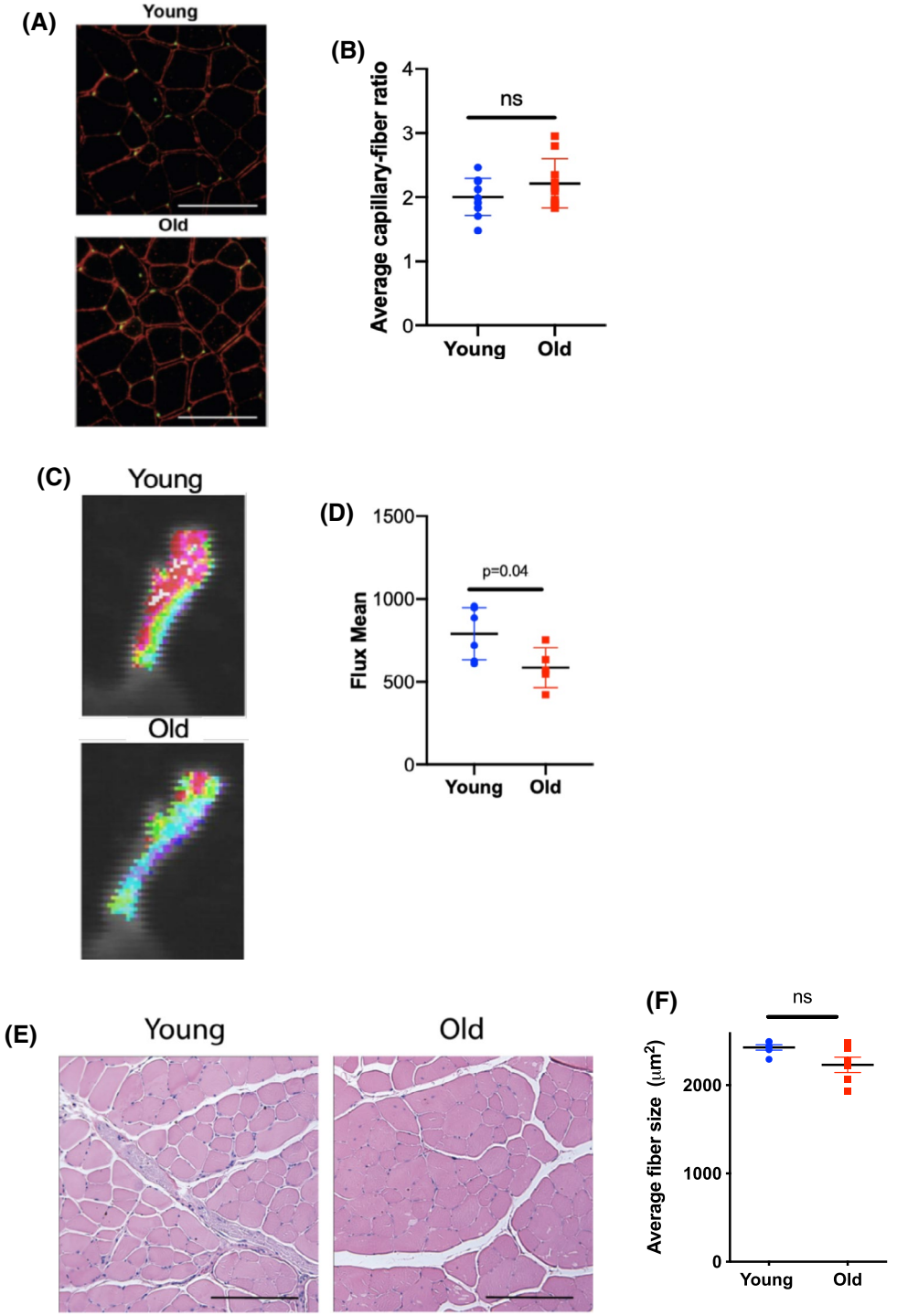

FIGURE 3 Blood flow, but not capillary density, is decreased in old mice. Immunofluorescent staining for CD31 (green) to identify capillaries and laminin (red) to outline the muscle fiber plasma membrane, demonstrated a similar capillary-to-fiber ratio in young and old mice (A,B, *Scale Bar* = 100 μm) (n = 8 per group), while blood flow at the hindlimb, as measured by doppler ultrasound, was significantly higher in young compared to old mice (C,D) (n = 5 per group). Baseline myofiber sizes are similar between young and old mice (E,F, Scale Bar: 200 μm) (n = 6 per group)

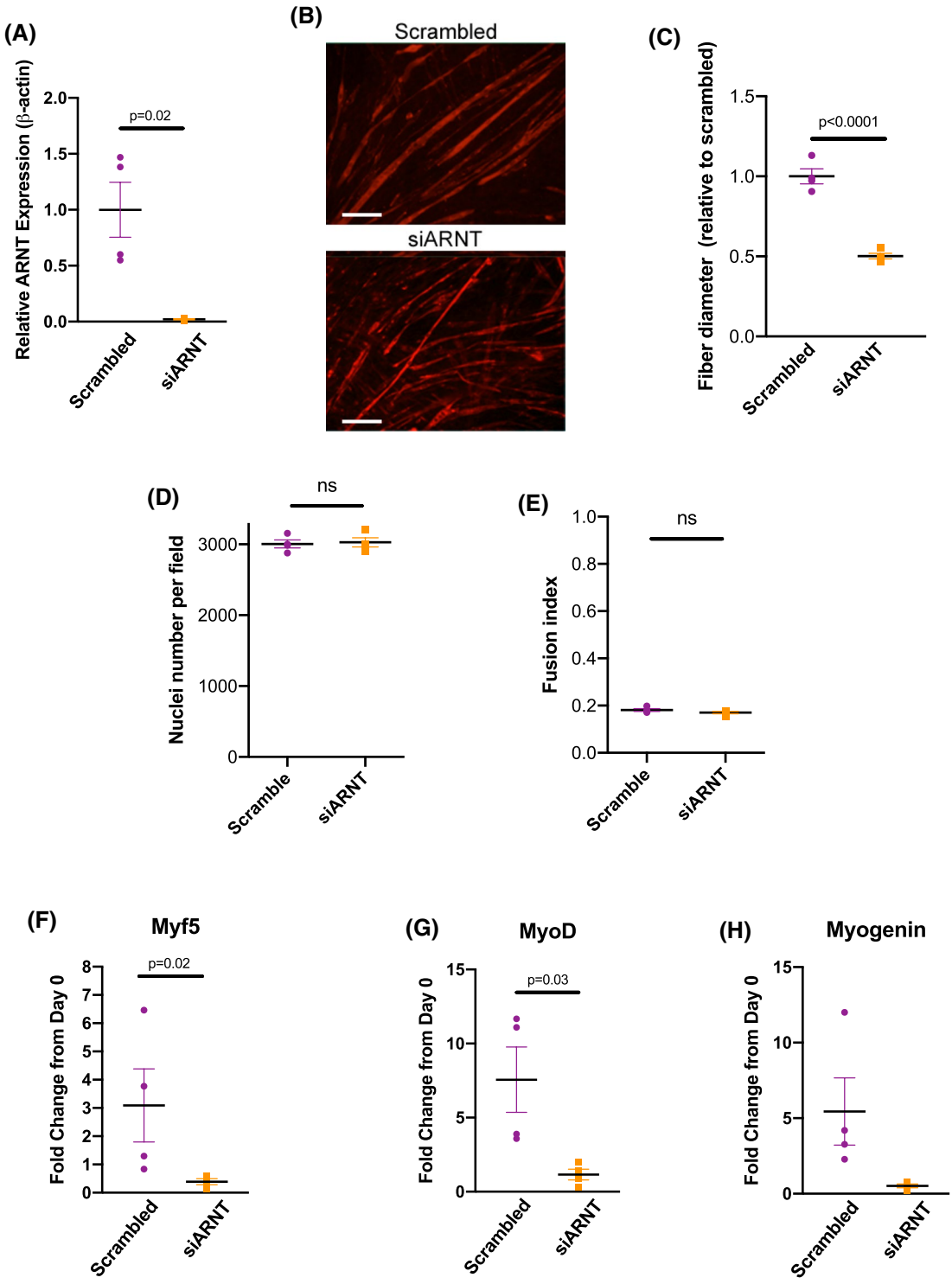

FIGURE 4 Knockdown of ARNT limits C2C12 differentiation. C2C12 primary muscle cells were treated with either scrambled siRNA, as a control, or siARNT (n = 4 per group). Treatment with siARNT resulted in a 98% decline of ARNT expression in comparison to the control group (A). Following 5 days of differentiation in a low-serum media and utilizing myosin heavy chain (MF20) to visualize muscle fibers, the mean diameter of the formed muscle fibers was 50% smaller in the siARNT-treated group compared to the scrambled siRNA-treated control group (B,C). Number of nuclei per high powered field (D) and fusion index (E) were similar between both groups. The gene expression of myogenic regulatory factors Myf5 (F) and MyoD (G) were significantly lower following ARNT siRNA treatment versus scrambled. No changes were observed in Myogenin gene expression following siARNT treatment (H). Scale Bar: 200 μm

impairs myogenesis, whether directly through its effect on Notch signaling or secondary to decreased blood flow.

3.3 | ARNT inhibition impairs myotube hypertrophy in a primary muscle cell line

To analyze the role of ARNT in myogenic differentiation in vitro, siRNA was utilized to knock down ARNT gene expression in differentiating C2C12 cells. Gene expression of ARNT was 98% lower in the siARNT-treated cells compared to the scrambled siRNA-treated control group ($P = .02$) (Figure 4A). The loss of *ARNT* impaired differentiation of C2C12 cells after 5 days in a low serum media under normoxia (Figure 4B,C). Specifically, ARNT knockdown resulted in abnormal fibers with a 50% decrease in myotube diameter ($P < .001$). There were no corollary changes in either the total cell number (Figure 4D) or fusion index (Figure 4E) following siARNT treatment. The gene expression of myogenic regulatory factors Myf5 ($P = .02$) and MyoD ($P = .03$) were significantly decreased following siARNT treatment (Figure 4F,G). No significant changes were detected in the myogenin gene expression (Figure 4H). This result is consistent with previous studies, which showed conversely that HIF-1α activation promotes the formation of hypertrophic myotubes.[19] Our findings further suggest that ARNT inhibition can directly impair myotube growth, even under normoxic conditions without the impairment of cellular number or fusion index.

3.4 | Muscle-specific ARNT knockout limits skeletal muscle regeneration in vivo

To determine whether ARNT is necessary for muscle regeneration in vivo, we utilized an inducible Cre-lox mouse model. $ARNT^{fl/fl}$ mice have previously demonstrated efficient knockout of ARNT in tissue-specific patterns.[20] We generated a compound, genetically modified mouse line by crossing $ARNT^{fl/fl}$ mice with the temporally regulatable, skeletal muscle-expressed human skeletal α-actin (HSA)-Cre ER transgene. This genetic system allows skeletal muscle-specific deletion of ARNT in its myotube and myofibers, but not in SMPs, upon injection of tamoxifen (Supporting Figure S2). Herein, the mice with the loss of ARNT expression in skeletal muscle will be referred to as muscle ARNT knockout (ARNT mKO), and the tamoxifen-treated littermate controls referred to as ARNT wild type (ARNT WT). Following activation, there were no differences noted in mouse weight or hind limb muscle mass between the ARNT mKO mice and littermate controls (Supporting Figure S2). The ARNT mKO mice exhibited 90% reduction in the skeletal muscle ARNT expression (Supporting Figure S2), similar to previous reports.[13] ARNT deletion in young mice hindered skeletal muscle regeneration in comparison to similarly treated littermate controls, as indicated by smaller regenerating muscle fibers on DPI 5 ($P < .001$) and DPI 10 ($P < .001$) in ARNT mKO mice (Figure 5A-C). Importantly, muscle-specific deletion of ARNT did not result in any decline in the proportion of SMPs within the muscle, or myogenic differentiation potential or fusion index following culture, thereby demonstrating the absence of intrinsic SMP defects in the ANRT mKO model (Figure 5D-H). This further suggests that the observed impairment in muscle regeneration in the ARNT mKO mice is due to the loss of ARNT signaling in the surrounding myofibers, and that the myogenic potential of SMPs is negatively affected by a niche effect resulting in delaying regenerative myogenesis.

3.5 | Skeletal muscle loss of ARNT decreases nuclear HIF-1α and N1ICD levels following injury

ARNT mKO mice exhibited no changes in skeletal muscle cytoplasmic HIF-1α levels but demonstrated a two-fold reduction in nuclear localization of HIF-1α at baseline ($P = .05$), DPI 5 ($P = .01$), and DPI 10 ($P = .03$) in comparison to ARNT WT mice (Figure 6A,B). Cytoplasmic ARNT protein levels in skeletal muscle harvested from ARNT mKO mice were similarly decreased at baseline ($P = .03$) and following injury ($P < .001$ on both DPI 5 and 10) (Figure 6C), as compared to ARNT WT mice. No changes were detected in nuclear ARNT levels between ARNT WT and mKO mice (Figure 6D). Immunofluorescence staining for ARNT further demonstrated decreased ARNT in the muscle fibers of the ARNT mKO mice in comparison to the littermate controls, without apparent changes in HIF-1α levels within muscle fibers (Figure 6E). Skeletal muscle harvested from ARNT mKO mice exhibited a twofold reduction in the N1ICD levels in the whole muscle as compared to ARNT WT ($P = .001$), similarly to the case of old vs young mice (Figure 6F,G). This loss of N1ICD in skeletal muscle suggests a potential mechanism by which the loss of ARNT limits muscle regeneration. Separately, ARNT WT and mKO mice without injury demonstrated no significant difference in the skeletal muscle capillary density (Figure 7A,B) or mid-thigh blood flow assessed by duplex ultrasound on day 10 following tamoxifen activation (Figure 7C,D). These findings suggest that the impaired muscle regeneration seen in the ARNT mKO mice was not likely dependent on vascular or perfusion changes within the muscle. Others have similarly demonstrated that constitutive skeletal muscle-specific knockout of ARNT inhibits hypoxia signaling without limiting vasculogenesis.[13]

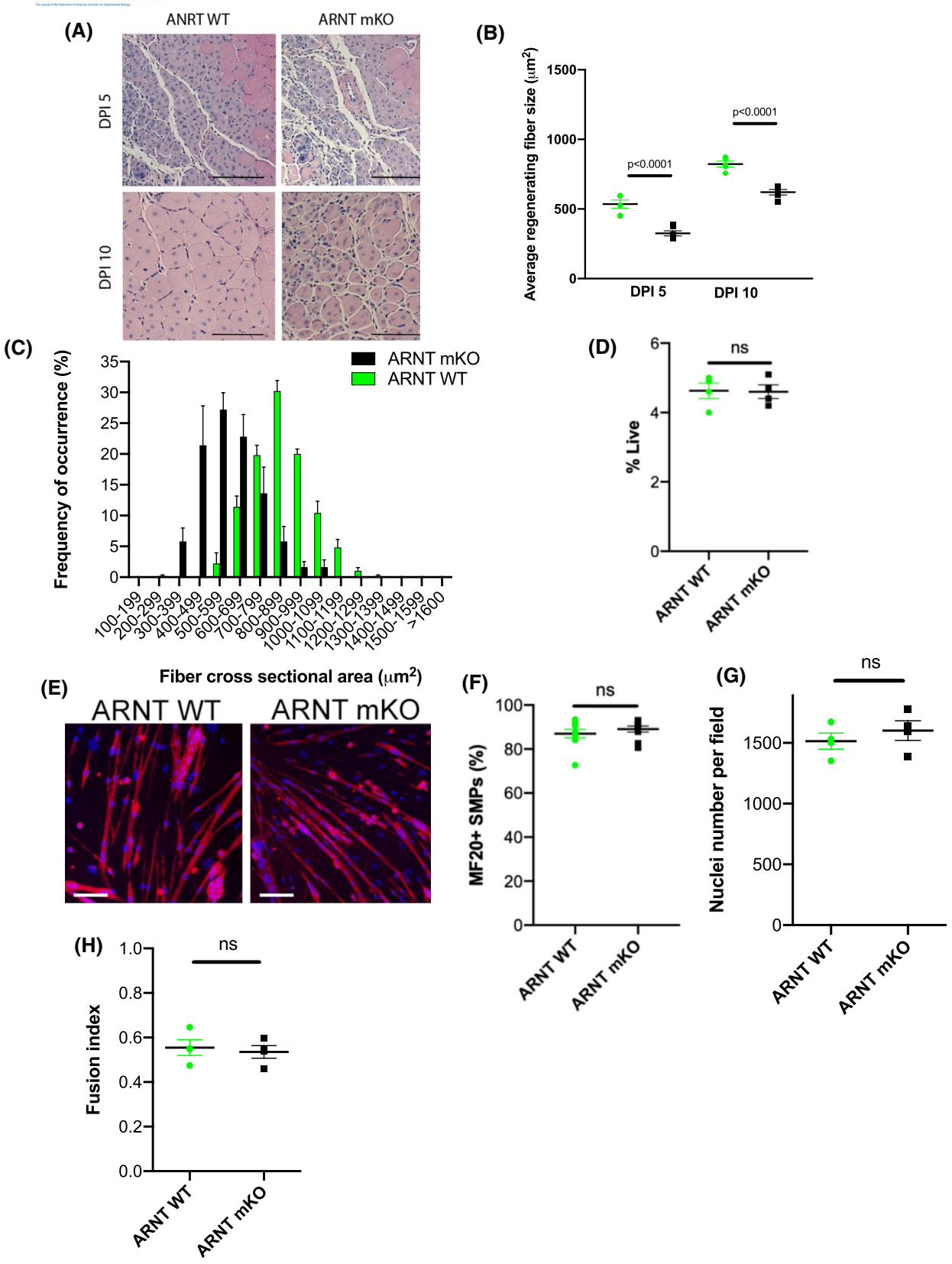

FIGURE 5 ARNT deletion impairs skeletal muscle regeneration following cryoinjury but not ex vivo SMP differentiation. Following cryoinjury to the TA, larger regenerating muscle fibers were observed on DPI 5 and 10 in ARNT WT as compared to ARNT mKO mice (A,B) (n = 4-6 per group). Frequency distribution of the cross-sectional area (CSA) of regenerating fibers demonstrates smaller regenerating fibers on DPI 10 (C) postinjury in the ARNT mKO mice. Flow cytometry was performed to isolate SMPs from the hind limb musculature of ARNT WT and ARNT mKO mice. Both groups exhibited similar frequency of SMP (n = 4) (D). In addition, the expression of myosin heavy chain (MF20) after 5 days in low-serum, differentiation media, was similar between the two groups (n = 6 per group) (E,F). Nuclei per field (G) and fusion index (H) were also similar between the two groups following 5 days in culture. Scale Bar: 200 μm

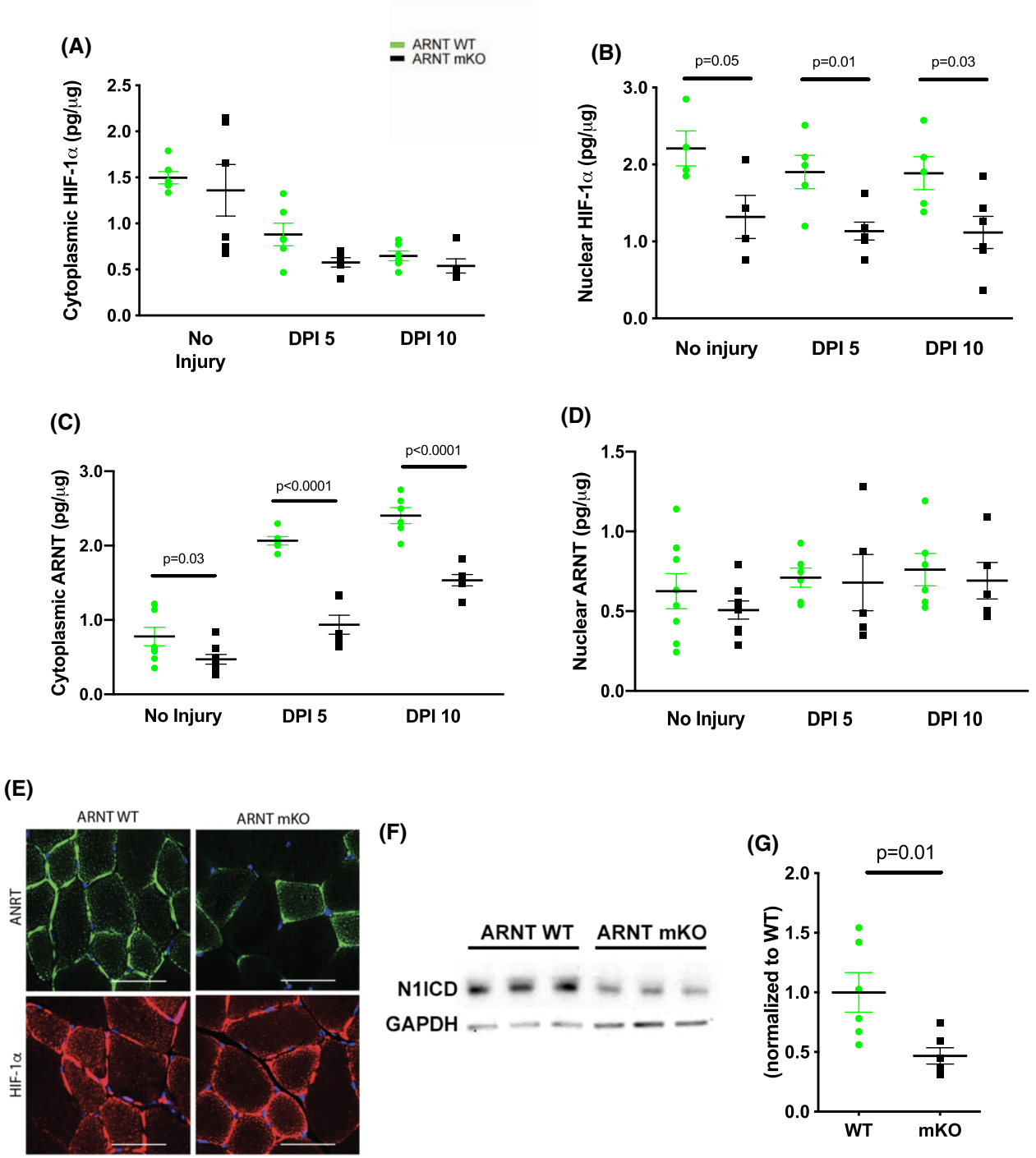

FIGURE 6 Nuclear levels of HIF-1α is decreased in in the ARNT mKO group. Cytoplasmic levels of HIF-1α were similar between ARNT WT and ARNT mKO mice, both at baseline and following injury (n = 4-6 per group) (A). In contrast, nuclear HIF-1α levels are consistently decreased in ARNT mKO mice as compared to littermate controls (n = 4-6 per group) (B). Cytoplasmic levels of ARNT were decreased in the muscle of ARNT mKO as compared to ARNT WT mice (C), whereas there were no differences in nuclear ARNT levels between the two groups (D) (n = 4-6 per group). Immunofluorescence staining demonstrates decreased ARNT in the mKO mice as compared to the littermate controls in uninjured, baseline fibers without apparent changes in muscle fiber HIF-1α (E). N1ICD levels were decreased in ARNT mKO mice compared to ARNT WT in uninjured muscle (F,G) (n = 6-8 per group). Scale Bar: 100 μm

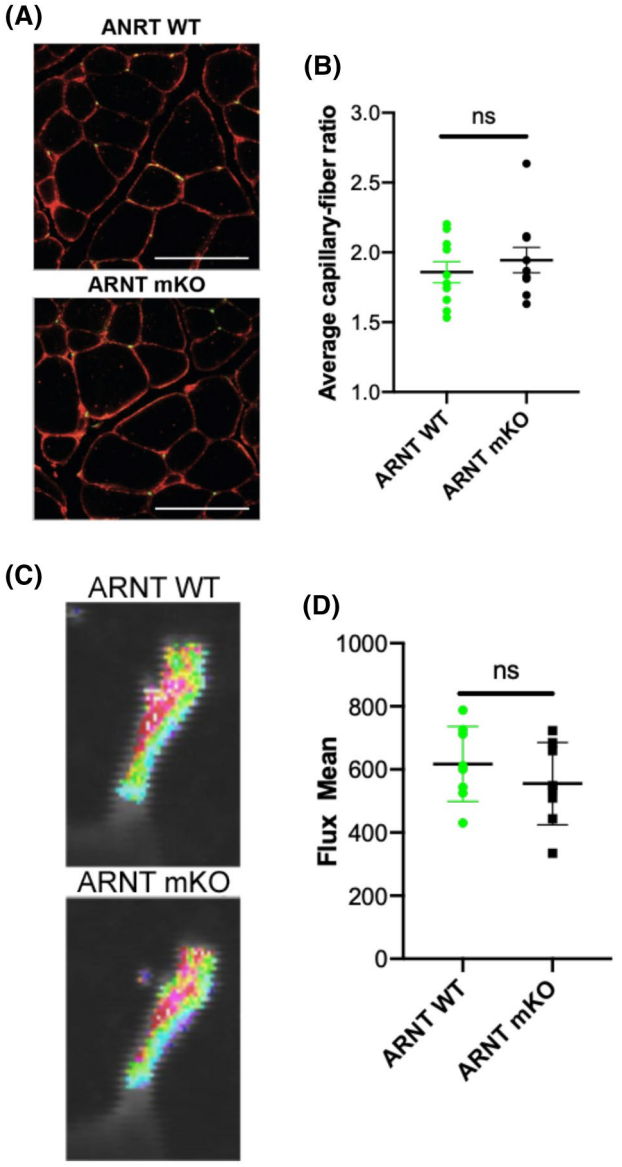

FIGURE 7 Blood flow and capillary density unaffected in ARNT mKO mice. Immunofluorescent staining of CD31 (green) to identify capillaries and laminin (red) to outline the muscle fiber plasma membrane, demonstrated a similar capillary-to-fiber ratio (A,B) (n = 8-10 per group) and doppler flow studies reported similar mid-thigh blood flow (C,D) between the ARNT WT and ARNT mKO mice (n = 8 per group). *Scale Bar* = 100 μm

3.6 | Administration of a hypoxia pathway activator improves muscle regeneration and augments HIF-1α translocation in old mice

ML228 is a small molecule inducer of the HIF-pathway, which does not inhibit prolyl hydroxylase domain (PHD) enzymes but instead promotes HIF1-α nuclear translocation and DNA binding.[21] Thus, it simulates the actions of ARNT. It has been previously shown that ML228 augments hypoxia signaling and HRE gene expression in vivo in a rodent model.[22] To assess the effects of the hypoxia pathway activation on skeletal muscle regeneration in aging, old mice were treated with either ML228 or a vehicle control (DMSO). ML228 was administered through intra-peritoneal injections once daily for 5 days (Figure 8A). The first injection was given on the day prior to the planned injury. Skeletal muscle was harvested on either 5 or 10 DPI. Separately, in order to assess the effects of ML228 treatment in uninjured muscle (baseline), ML228 or DMSO was injected once daily for 5 days and uninjured skeletal muscle was harvested after 10 days. Marginally lower levels of cytoplastic HIF-1α were observed on DPI 10 in the ML228-treated group (Figure 8B). ML228 administration resulted in 75% increase in the nuclear HIF-1α at baseline ($P = .05$) and nearly 100% increase on both DPI 5 ($P = .04$) and 10 ($P = .02$) as compared to the mice treated with vehicle control (Figure 8C). This was accompanied by a fivefold increase in the whole muscle N1ICD levels in the ML228-treated old mice compared to the vehicle-treated old mice (Figure 8D,E).

The old mice treated with ML228 exhibited 40% increase in CSA of regenerating fibers on DPI 5 and 100% increase by DPI 10 ($P < .001$) (Figure 9A-C) in comparison to the old mice treated with vehicle control. No differences were found in the mid-thigh blood flow, capillary density, or baseline, uninjured muscle fiber CSA between the two groups (Supporting Figure S3). In order to determine whether ML228 improved skeletal muscle regeneration via induction of hypoxia signaling, ARNT WT and mKO mice were similarly treated with either ML228 or DMSO. One week following the tamoxifen administration, the mice were treated with either ML228 or control once daily for 5 days. These mice underwent cryoinjury on the second day of ML228 injection, similarly to the old mice as described above. ML228 administration improved regenerating muscle fiber CSA by 25% on DPI 10 in the ARNT mKO mice ($P < .001$) compared to the ARNT mKO mice treated with vehicle control. Muscle regeneration in ARNT WT mice was unaffected by the ML228 treatment (Figure 9D,E). No differences in either skeletal muscle regeneration or HIF levels were observed following the ML228 supplementation in young mice compared to their vehicle-treated littermate controls, suggesting that the response to ML228 is age-specific (Supporting Figure S4).

To evaluate whether N1ICD was necessary for ML228-induced improvement in skeletal muscle regeneration in aging, old mice were treated with either vehicle control, ML228, DAPT, or ML228 and DAPT concurrently. DAPT, a γ-secretase inhibitor, limits Notch signaling by preventing the conversion of Notch1 to N1ICD.[23] In old mice, treatment with DAPT alone resulted in similar N1ICD levels as compared to DMSO treatment. ML228 treatment resulted in a threefold increase in whole muscle N1ICD levels ($P = .003$), similarly to the previous experiment. In old mice, concurrent treatment with ML228 and DAPT reduced N1ICD levels by approximately 30% compared to ML228 treatment alone

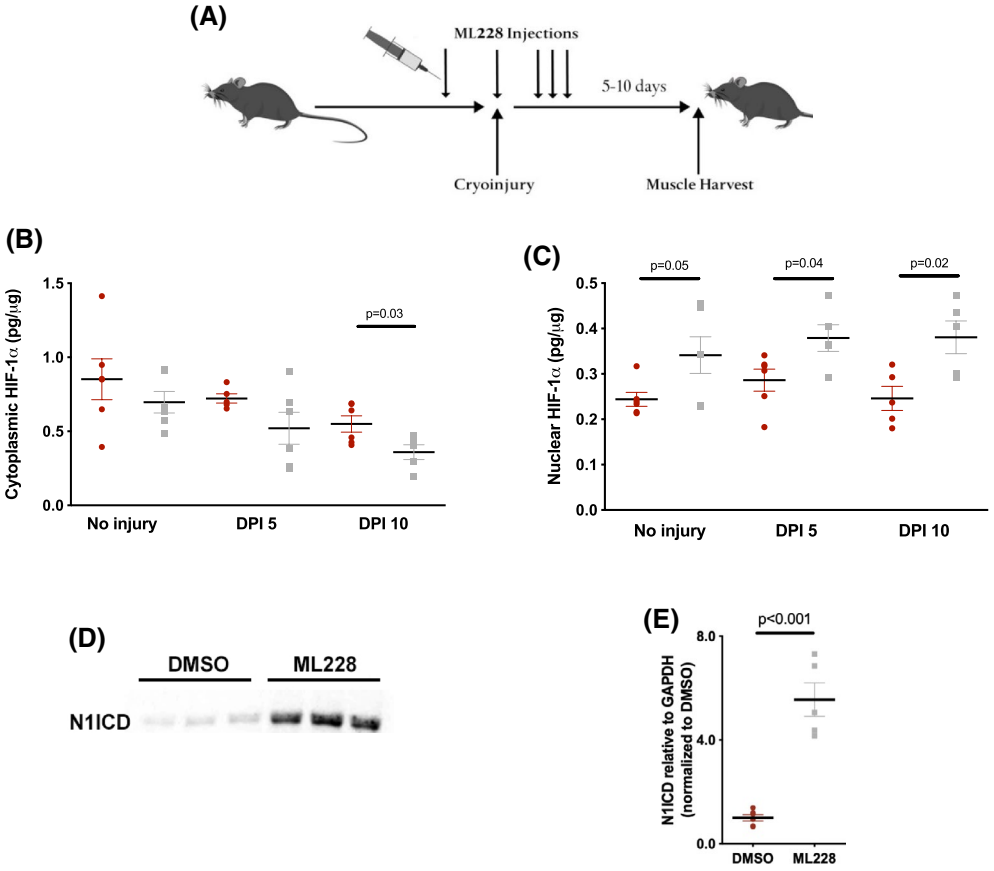

FIGURE 8 ML228 supplementation improves hypoxia signaling. Old mice (23-25 months) were given injections of a pharmacological hypoxia pathway activator, ML228, or a vehicle control, DMSO, for five consecutive days (schematic represented in A). In the mice with no injury, skeletal muscle was harvested 5 or 10 days following the last ML228 injection (n = 5-6 per group). Cytoplasmic HIF-1α levels were similar following ML228 versus vehicle administration in skeletal muscle from old mice (n = 5-6 per group) (B). The nuclear levels of HIF-1α (C) and whole muscle N1ICD (D,E) were significantly higher in the ML228 versus vehicle-treated old mice (n = 5-6 per group)

($P = .04$, Figure 10A,B). Treatment with DAPT given with ML228 also abrogated the increase in regenerating fiber CSA in seen with the treatment with ML228 alone in old mice (Figure 10C,D).

4 | DISCUSSION

SMPs are required for postnatal skeletal muscle growth and recovery following injury.[24,25] Several factors have been implicated as a cause of decline in muscle regeneration with aging, including the changes in the muscle stem cell niche.[6] Here, we report that cytoplasmic ARNT levels and hypoxia signaling are diminished in old skeletal muscle, and restoring them improves myogenesis, possibly through their effects on the whole skeletal muscle levels of N1ICD. Interestingly, although hypoxia signaling is associated with changes in angiogenesis and blood flow, our data suggest that there are, in addition, some direct effects of ARNT-mediated hypoxia-signaling on muscle regeneration. Mice with a skeletal muscle-specific deletion of ARNT exhibited decreased levels of N1ICD and impairment in skeletal muscle regeneration. Similarly, ML228 supplementation in old mice restored N1ICD levels and skeletal muscle regeneration without changes in capillary density or blood flow at the time points tested. The addition of DAPT, an inhibitor of Notch signaling, decreased the benefit on muscle regeneration conferred by ML228 treatment in old mice, suggesting that N1ICD may be partially responsible for the hypoxia signaling-mediated improvements in muscle regeneration.

The regulation of ARNT levels and why it changes with aging are unclear, although the ARNT gene expression was noted to be significantly decreased with aging. Notably, such changes in ARNT levels and hypoxia signaling in general may be due to genomic instability, epigenetic changes, or loss of protein homeostasis.[26] Further investigation into the differential regulation of ARNT with aging is necessary to understand why ARNT gene expression and protein levels decreases with aging. Of note, with regards to ARNT deletion within skeletal muscle fibers, the loss of hypoxic response in injured myocytes may limit muscle regeneration

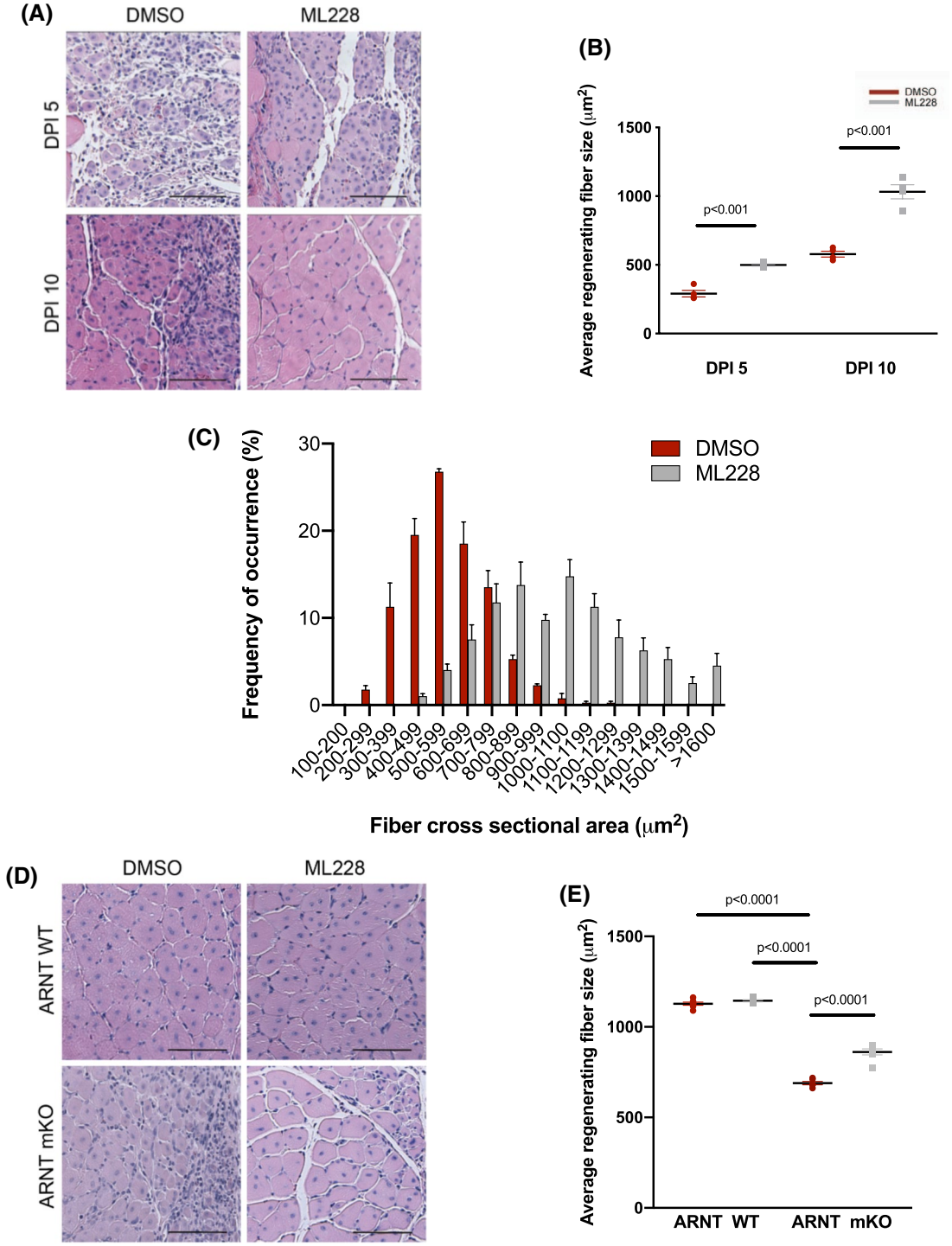

FIGURE 9 Administration of ML228 improves muscle regeneration in aging. Old mice underwent treatment with five daily doses of ML228 IP injection, starting on the day prior to cryoinjury. The TA muscle of old mice treated with ML228 demonstrated increased regenerating fiber CSA versus similarly old, vehicle-treated mice on DPI 5 and 10 (A-C) (n = 4 per group). ML228 treatment of ARNT mKO but not ARNT WT mice improved regenerating fiber CSA on DPI 10 (D,E) (n = 5 per group). Scale Bar: 200 μm

secondary to decreased levels of N1ICD and activation of SMPs. However, this does not preclude the possibility that skeletal muscle stem cells may also be limited in their ability to differentiate. As skeletal muscle stem cells form nascent, mature fibers, they will express α-skeletal actin and, thereby, lose ARNT gene expression in our mouse model. As such, differentiation may be limited within these myofibers and thus decrease regenerating fiber size following injury.

The role of hypoxia signaling and HIF activity in response to muscle injury remains unclear. Skeletal muscle

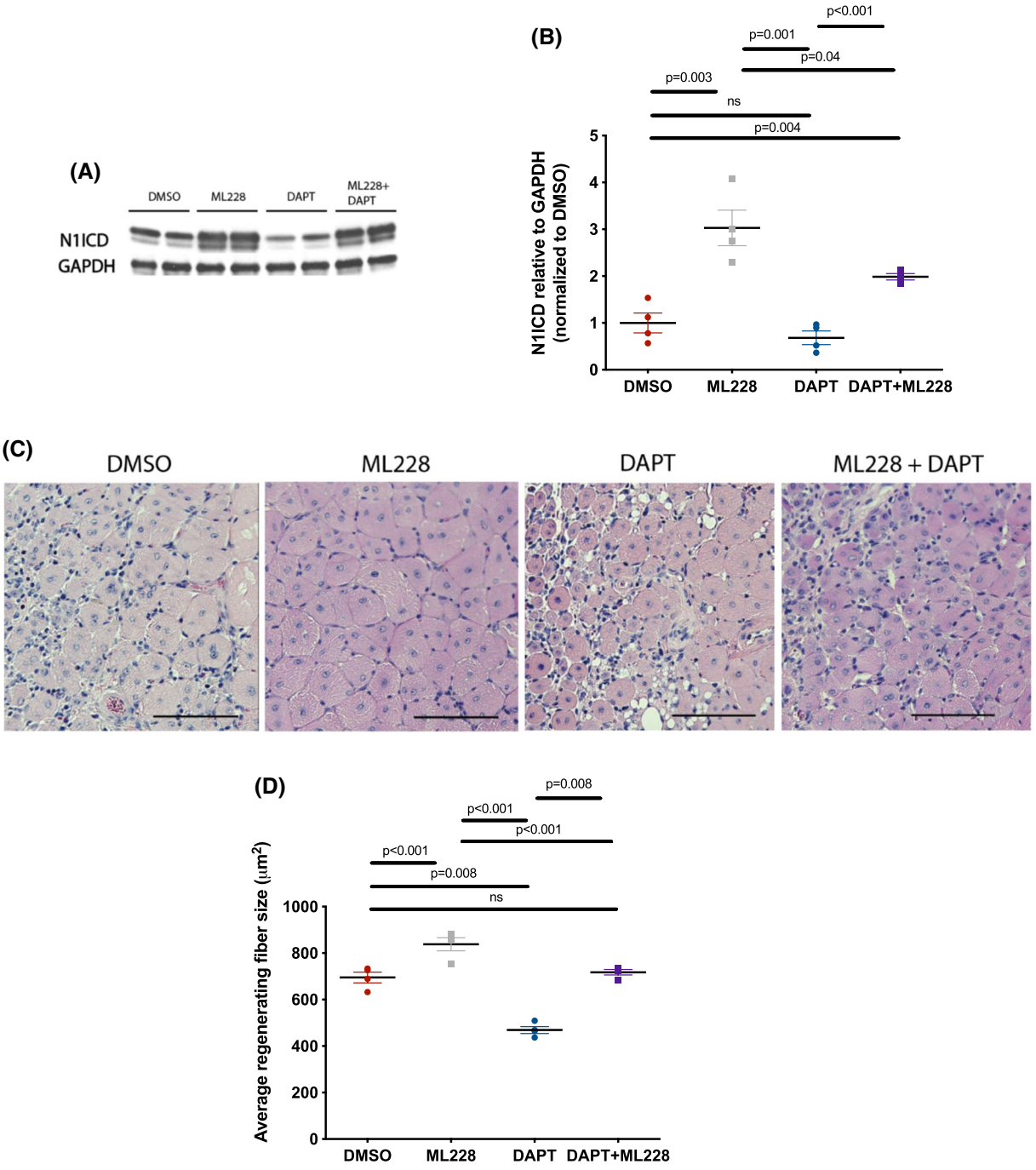

FIGURE 10 Concurrent administration of DAPT limits ML228 induced improvement in muscle regeneration in aging. Old mice underwent treatment with five daily doses of vehicle control (DMSO), ML228, DAPT, or ML228 and DAPT IP injection, starting on the day before cryoinjury. N1ICD levels were highest in the ML228-treated group, but decrease with administration of DAPT in combination with ML228 (n = 4 per group) (Figure 10A,B). The TA muscle of old mice treated with ML228 demonstrated increased regenerating fiber CSA versus similarly old, vehicle-treated mice on DPI 10 (C, D). Treatment with DAPT combined with ML228 limited improved regenerating fiber CSA seen in the treatment with ML228 alone (n = 4 per group). Scale Bar: 200 μm

stem cells exist in a hypoxic niche and are themselves intracellularly hypoxic.[27] The regulation of hypoxia signaling factors are important determinant of myogenesis by skeletal muscle stem cells, although their roles are complex.[28] Majumdar and colleagues previously demonstrated that while loss of HIF-1α in Pax3-expressing muscle precursors does not alter muscle development, loss of HIF-1α expression in Pax7-expressing precursors in adulthood accelerates skeletal muscle regeneration following injury.[29] Similarly, transient, systemic inhibition of HIF-2α promotes skeletal muscle regeneration following cardiotoxin injury.[27] However, others have demonstrated the benefits

of hypoxia signaling on myogenesis. Cirillo and colleagues reported that activation of HIF-1α promotes myogenesis and fiber hypertrophy through a noncanonical Wnt pathway in a primary cell line.[19] Separately, combined deletion of HIF-1α and HIF-2α expression in muscle stem cells restrained skeletal muscle regeneration following injury.[9] PHD2 inhibition resulting in augmented hypoxia signaling similarly improves muscle regeneration in a murine model of obesity.[30] Regulation of particular HIFs may indeed have differential effects and may account for some of the differences demonstrated in these previous studies.[31]

Our study focused on the niche effect of hypoxia signaling and ARNT on myogenesis. Aging alters the microenvironmental niche, which has been associated with limited stem cell proliferation and activity.[32,33] Age-related muscle wasting, in particular, is linked to decline of SMP number and myogenic potential, as a result of changes within the niche.[34,35] Our study suggests that age-related loss of ARNT expression in myofibers readily limits regenerative potential as a niche effect, as supported by the results that SMPs isolated from ARNT mKO muscle differentiated similarly to SMPs harvested from wild-type mice ex vivo, although cell intrinsic changes in SMPs cannot be entirely excluded. Loss of Notch within the stem cell niche underlies aging-associated decline in myogenesis,[14] and limits regeneration following injury when specifically deleted from myofibers.[7] Our study is in agreement with previous reports suggesting that hypoxia signaling regulates Notch levels.[5,36] In our study, loss of ARNT in the cytoplasm of skeletal muscle fibers reduced N1ICD levels, while ML228 administration increased the whole muscle N1ICD in the context of similar levels of cytoplasmic HIF-1α. Dysregulation in ARNT-mediated regulation of Notch signaling within the niche is, therefore, a potential mechanism explaining the loss of myogenic potential in aging. It is also important to note that supplementation of hypoxia signaling improved myogenesis and Notch activity in the absence of increased capillary density or blood flow, which may otherwise increase regenerative capacity and stem cell number.[37] The role of nuclear ARNT, which was unchanged between skeletal muscle from young and old mice, is unclear from our study and further research is necessary to determine if it may have a role in regulating muscle regeneration. In addition, although ARNT staining was evident within muscle fibers, we cannot exclude that other cell types may express ARNT and thereby modulate muscle regeneration.

Taken together, our data suggest that hypoxia signaling in skeletal muscle declines with aging in part due to the loss of ARNT. Pharmacological activation of hypoxia signaling with ML228 supplementation does not further enhance skeletal muscle regeneration in young, wild-type mice, suggesting that rescuing the hypoxia signaling pathway restores muscle regeneration only in the context of pathologically low levels of ARNT. The varied response to injury vis-à-vis ARNT levels in young and old mice sheds a new insight into its role in the maintenance of nuclear HIF levels, and thus, hypoxia signaling during regenerative responses. The loss of such ARNT responses to injury in old muscle may, as such, contribute to the age-related decline in muscle regeneration.

ACKNOWLEDGMENTS

We thank Teri Bowman of the Dana-Farber/Harvard Cancer Center Specialized Histopathology Core for histology services, Shayan Olumi for histological analysis, Alison Marotta and Angela Wood of the Joslin Flow Cytometry core for flow cytometry, and Farzana Hakim of the Joslin iPS core with assistance in cell culture. $ARNT^{fl/fl}$ mice were a kind gift of Dr Frank Gonzalez at the National Institutes of Health and human skeletal muscle Cre mice were a kind gift of Dr William Kaelin at the Dana Farber Cancer Institute. This work was supported by the National Institute of Aging (K76AG059996 to IS), the National Institute of Diabetes and Digestive and Kidney Diseases (P30 DK036836 to AJW), the Glenn Foundation for Medical Research (AJW), and a Research and Education Committee Grant (IS) from the Boston Claude D. Pepper Center, which is funded by the National Institute of Aging (P30AG031679 to SB).

CONFLICT OF INTEREST

The authors have declared that no conflict of interest exists.

AUTHOR CONTRIBUTIONS

Y. Endo, K. Baldino, YE, B. Li, Y. Zhang, D. Sakthivel, M. MacArthur, A. Panayi, P. Kip, D.J. Spencer, R. Jasuja, D. Bagchi, R.L. Neppl, K. Nuutila, and I. Sinha designed research studies, conducted experiments, acquired data, and analyzed data. YE and IS and wrote the manuscript. S. Bhasin, K. Nuutila, R.L. Neppl, A.J. Wagers, and I. Sinha supervised and designed research studies, analyzed data, and revised the manuscript.

REFERENCES

1. Cerletti M, Jurga S, Witczak C, et al. Highly efficient, functional engraftment of skeletal muscle stem cells in dystrophic muscles. *Cell*. 2008;134(1):37-47. https://doi.org/10.1016/j.cell.2008.05.049
2. Feige P, Brun C, Ritso M, Rudnicki M. Orienting muscle stem cells for regeneration in homeostasis, aging, and disease. *Cell Stem Cell*. 2018;23(5):653-664. https://doi.org/10.1016/j.stem.2018.10.006
3. Liu W, Wen Y, Bi P, et al. Hypoxia promotes satellite cell self-renewal and enhances the efficiency of myoblast transplantation. *Development*. 2012;139(16):2857-2865. https://doi.org/10.1242/dev.079665
4. Chakravarthy M, Spangenburg E, Booth F. Culture in low levels of oxygen enhances in vitro proliferation potential of satellite cells from old skeletal muscles. *Cell Mol Life Sci*. 2001;58(8):1150-1158. https://doi.org/10.1007/pl00000929

5. Gustafsson M, Zheng X, Pereira T, et al. Hypoxia requires notch signaling to maintain the undifferentiated cell state. *Dev Cell*. 2005;9(5):617-628. https://doi.org/10.1016/j.devcel.2005.09.010
6. Conboy I, Conboy M, Wagers A, Girma E, Weissman I, Rando T. Rejuvenation of aged progenitor cells by exposure to a young systemic environment. *Nature*. 2005;433(7027):760-764. https://doi.org/10.1038/nature03260
7. Bi P, Yue F, Sato Y, et al. Stage-specific effects of Notch activation during skeletal myogenesis. *Elife*. 2016;5:e17355. https://doi.org/10.7554/elife.17355
8. Liu L, Charville G, Cheung T, et al. Impaired notch signaling leads to a decrease in p53 activity and mitotic catastrophe in aged muscle stem cells. *Cell Stem Cell*. 2018;23(4):544-556.e4. https://doi.org/10.1016/j.stem.2018.08.019
9. Yang X, Yang S, Wang C, Kuang S. The hypoxia-inducible factors HIF1α and HIF2α are dispensable for embryonic muscle development but essential for postnatal muscle regeneration. *J Biol Chem*. 2017;292(14):5981-5991. https://doi.org/10.1074/jbc.m116.756312
10. Eltzschig H, Bratton D, Colgan S. Targeting hypoxia signalling for the treatment of ischaemic and inflammatory diseases. *Nat Rev Drug Discovery*. 2014;13(11):852-869. https://doi.org/10.1038/nrd4422
11. Mandl M, Depping R. Hypoxia-inducible aryl hydrocarbon receptor nuclear translocator (ARNT) (HIF-1β): is it a rare exception? *Mol Med*. 2014;20(1):215-220. https://doi.org/10.2119/molmed.2014.00032
12. Maltepe E, Schmidt J, Baunoch D, Bradfield C, Simon M. Abnormal angiogenesis and responses to glucose and oxygen deprivation in mice lacking the protein ARNT. *Nature*. 1997;386(6623):403-407. https://doi.org/10.1038/386403a0
13. Badin P, Sopariwala D, Lorca S, Narkar V. Muscle Arnt/Hif1β is dispensable in myofiber type determination, vascularization and insulin sensitivity. *PLoS One*. 2016;11(12):e0168457. https://doi.org/10.1371/journal.pone.0168457
14. Conboy I. Notch-mediated restoration of regenerative potential to aged muscle. *Science*. 2003;302(5650):1575-1577. https://doi.org/10.1126/science.1087573
15. Engin F, Bertin T, Ma O, et al. Notch signaling contributes to the pathogenesis of human osteosarcomas. *Hum Mol Genet*. 2009;18(8):1464-1470. https://doi.org/10.1093/hmg/ddp057
16. Oh J, Sinha I, Tan K, et al. Age-associated NF-κB signaling in myofibers alters the satellite cell niche and re-strains muscle stem cell function. *Aging (Albany NY)*. 2016;8(11):2871-2896. https://doi.org/10.18632/aging.101098
17. Hardy D, Besnard A, Latil M, et al. Comparative study of injury models for studying muscle regeneration in mice. *PLoS ONE*. 2016;11(1):e0147198. https://doi.org/10.1371/journal.pone.0147198
18. Hendrickse P, Degens H. The role of the microcirculation in muscle function and plasticity. *J Muscle Res Cell Motil*. 2019;40(2):127-140. https://doi.org/10.1007/s10974-019-09520-2
19. Cirillo F, Resmini G, Ghiroldi A, et al. Activation of the hypoxia-inducible factor 1a promotes myogenesis through the noncanonical Wnt pathway, leading to hypertrophic myotubes. *FASEB J*. 2017;31(5):2146-2156. https://doi.org/10.1096/fj.201600878r
20. Tomita S, Sinal C, Yim S, Gonzalez F. Conditional disruption of the aryl hydrocarbon receptor nuclear translocator (Arnt) gene leads to loss of target gene induction by the Aryl hydrocarbon receptor and hypoxia-inducible factor 1α. *Mol Endocrinol*. 2000;14(10):1674-1681. https://doi.org/10.1210/mend.14.10.0533
21. Theriault J, Felts A, Bates B, et al. Discovery of a new molecular probe ML228: an activator of the hypoxia inducible factor (HIF) pathway. *Bioorg Med Chem Lett*. 2012;22(1):76-81. https://doi.org/10.1016/j.bmcl.2011.11.077
22. Chen H, Li J, Liang S, et al. Effect of hypoxia-inducible factor-1/vascular endothelial growth factor signaling pathway on spinal cord injury in rats. *Exp Ther Med*. 2017;13(3):861-866. https://doi.org/10.3892/etm.2017.4049
23. Takeshita K, Satoh M, Ii M, et al. Critical role of endothelial Notch1 signaling in postnatal angiogenesis. *Circ Res*. 2007;100(1):70-78. https://doi.org/10.1161/01.res.0000254788.47304.6e
24. Pawlikowski B, Pulliam C, Betta N, Kardon G, Olwin B. Pervasive satellite cell contribution to uninjured adult muscle fibers. *Skelet Muscle*. 2015;5(1):42. https://doi.org/10.1186/s13395-015-0067-1
25. Sambasivan R, Yao R, Kissenpfennig A, et al. Pax7-expressing satellite cells are indispensable for adult skeletal muscle regeneration. *Development*. 2011;138(17):3647-3656. https://doi.org/10.1242/dev.067587
26. Yeo E. Hypoxia and aging. *Exp Mol Med*. 2019;51(6):1-15. https://doi.org/10.1038/s12276-019-0233-3
27. Xie L, Yin A, Nichenko A, Beedle A, Call J, Yin H. Transient HIF2A inhibition promotes satellite cell proliferation and muscle regeneration. *Journal of Clinical Investigation*. 2018;128(6):2339-2355. https://doi.org/10.1172/jci96208
28. Huang X, Trinh T, Aljoufi A, Broxmeyer H. Hypoxia signaling pathway in stem cell regulation: good and evil. *Curr Stem Cell Rep*. 2018;4(2):149-157. https://doi.org/10.1007/s40778-018-0127-7
29. Majmundar A, Lee D, Skuli N, et al. HIF modulation of Wnt signaling regulates skeletal myogenesis in vivo. *Development*. 2015;142(14):2405-2412. https://doi.org/10.1242/dev.123026
30. Sinha I, Sakthivel D, Olenchock B, et al. Prolyl hydroxylase domain-2 inhibition improves skeletal muscle regeneration in a male murine model of obesity. *Front Endocrinol (Lausanne)*. 2017;8:https://doi.org/10.3389/fendo.2017.00153
31. Keith B, Johnson R, Simon M. HIF1α and HIF2α: sibling rivalry in hypoxic tumour growth and progression. *Nat Rev Cancer*. 2011;12(1):9-22. https://doi.org/10.1038/nrc3183
32. Chakkalakal J, Jones K, Basson M, Brack A. The aged niche disrupts muscle stem cell quiescence. *Nature*. 2012;490(7420):355-360. https://doi.org/10.1038/nature11438
33. DeCarolis N, Kirby E, Wyss-Coray T, Palmer T. The Role of the Microenvironmental Niche in Declining Stem-Cell Functions Associated with Biological Aging. *Cold Spring Harb Perspect Med*. 2015;5(12):a025874. https://doi.org/10.1101/cshperspect.a025874.
34. Sacco A, Puri P. Regulation of muscle satellite cell function in tissue homeostasis and aging. *Cell Stem Cell*. 2015;16(6):585-587. https://doi.org/10.1016/j.stem.2015.05.007
35. Brack A, Conboy M, Roy S, et al. Increased Wnt signaling during aging alters muscle stem cell fate and increases fibrosis. *Science*. 2007;317(5839):807-810. https://doi.org/10.1126/science.1144090
36. Sahlgren C, Gustafsson M, Jin S, Poellinger L, Lendahl U. Notch signaling mediates hypoxia-induced tumor cell migration and invasion. *Proc Natl Acad Sci U S A*. 2008;105(17):6392-6397. https://doi.org/10.1073/pnas.0802047105
37. Verma M, Asakura Y, Murakonda B, et al. Muscle satellite cell cross-talk with a vascular niche maintains quiescence via VEGF

and notch signaling. *Cell Stem Cell*. 2018;23(4):530-543.e9. https://doi.org/10.1016/j.stem.2018.09.007

SUPPORTING INFORMATION

Additional Supporting Information may be found online in the Supporting Information section.

How to cite this article: Endo Y, Baldino K, Li B, et al. Loss of ARNT in skeletal muscle limits muscle regeneration in aging. *The FASEB Journal*. 2020;34: 16086–16104. https://doi.org/10.1096/fj.202000761RR